Available online at www.derpharmachemica.com

Scholars Research Library

Der Pharma Chemica, 2015, 7(10):186-201
(http://derpharmachemica.com/archive.html)

ISSN 0975-413X
CODEN (USA): PCHHAX

Synthesis, spectroscopic characterization and DNA interaction of schiff base curcumin Cu(II), Ni(II) and Zn(II) complexes

Priyadharshini N, Iyyam Pillai S[1], Subramanian S[2] and P. Venkatesh[1*]

[1]P.G and Research Department of Chemistry, Pachaiyappa's College, Chennai, Tamilnadu, India
[2]Department of Biochemistry, University of Madras, Guindy Campus, Chennai, Tamilnadu, India

---

ABSTRACT

A series of Cu(II), Ni(II) and Zn(II) complexes have been synthesized with newly synthesized Schiff base derived from curcumin and hydrazine hydrate. The structural features have been arrived from their FT-IR, ^{1}H NMR, ^{13}C NMR, mass, UV-vis spectroscopic studies. The binding behaviours of the synthesis complexes towards calf thymus DNA have been investigated by absorption spectra, emission spectra, viscosity measurements and circular dichroic studies. The DNA binding constants reveal that all these complexes interact with DNA via intercalating binding mode with binding constants (K_b) of 5.01 x 10^4 M^{-1}, 4.61 x 10^4 M^{-1} and 4.38 x 10^4 M^{-1} and K_{app} of 6.04 x 10^5 M^{-1}, 5.72 x 10^5 M^{-1} and 5.46 x 10^5 M^{-1}.

Keywords: Curcumin, DNA binding, Viscosity, Intercalation, hydrazine hydrate.

INTRODUCTION

The need to improve drug design for minimizing the toxic side effects and understand the mechanism of biological reactions has given a thrust for continuous research in medicinal inorganic chemistry. In drug design, targeting is an important phenomenon because; toxicity is often encountered only if the drugs are not delivered to the specific tissues, cells and receptors where they are required. If the active species of drugs contain metal complexes, then the complexes can spontaneously undergo biological reactions such as ligand substitution and redox reactions. Thus, enumerating the mechanism of the active species on biological reactions is expected to yield valuable information about using the metal complexes as drugs [1]. In the field of medicinal research, Schiff base metal complexes of mixed aromatic ligands are the main focus for the development of new therapeutic agents [2]. The interaction of transition metal complexes with DNA has been a subject of passionate research in the field of bioinorganic chemistry, ever since the discovery of cis-platin as an anticancer agent. As an important intention of anticancer drugs, DNA plays a central role in replication, transcription, and regulation of genes. DNA has strong affinity towards many organic compounds and transition metal complexes. In its polyionic form, DNA can attract any cationic species and also neutral organic compounds. These compounds may react with or bind to DNA with high affinity and cause the decay of cell at an appropriate time [3]. Many studies indicate that transition metal complexes can interact non-covalently with DNA by intercalation, groove binding, or external electrostatic binding [4]. Many important applications of these complexes require that they could bind to DNA in an intercalative mode [5]. However, while groove binding determines only little deviations in the B-form structure of the DNA double helix, the intercalation mode induces the most dramatic changes in the DNA structure [6]. Molecules with extended planar aromatic systems can be inserted between paired DNA bases through π-π stacking so as to afford significant unwinding, stiffening and lengthening of the helix. This is why intercalators can transcend resistance phenomena common to other drugs [7,8]. Hence, it is very important to develop compounds with both strong antioxidant and DNA-binding properties for effective cancer therapy. The specific roles of ligands analogous to the molecules that bind to or modulate the function of biological receptors make them good candidates for drug development. In recent

years, the design and synthesis of new ligands with combined biological, structural and coordination properties have burgeoned. Interest in these studies stems not only from the different coordination modes but also from their chemical reactivity. Hydrazine derivatives containing N-heterocycles and their complexes exhibit strong antitumor and antivirus activities [9,10]. Curcumin(1,7-bis(4-hydroxy-3-methoxyphenyl)-1,6 heptadiene -3,5-dione;) is an important natural phytochemical compound found in the rhizomes of Curcuma longa or turmeric, which has been used in China to treat digestive and neuropsychiatric disorders [11]. The medicinal activity of curcumin has been known since ancient times. It has also been used as a photodynamic agent useful for the destruction of bacteria and tumor cells. Multiple therapeutic activities have been attributed to curcumin mostly because of its anti-inflammatory and anti-oxidant effects. As such, curcumin was predominantly used to treat inflammatory conditions including bronchitis, colds, parasitic worms, leprosy, arthritis and inflammations of bladder, liver, kidney and skin, and to improve symptoms such as fever and diarrhea. In addition, curcumin is thought to have beneficial effects in diseases of the neurological system including Alzheimer's disease [12].

However, the structural and biological properties of hydrazone transition metal complexes derived from curcumin and salicylaldehyde have not been explored well. This aroused our interest in the synthesis of the ligand L, and its copper(II), Zinc(II) and Nickel(II) complexes with a view towards evaluating their structure activity relationship on biological property as DNA binding.

MATERIALS AND METHODS

2.1. Reagents and instruments

All reagents, curcumin, salicylaldehyde, hydrazine hydrate and metal(II) chlorides were of Merck products and they were used as supplied. Commercial solvents were distilled and then used for the preparation of ligands and their complexes. DNA was purchased from Bangalore Genei (India). Tris(hydroxymethyl)aminomethane–HCl (Tris–HCl) buffer solution was prepared using deionized and sonicated triple distilled water. The IR spectral studies were carried out in the solid state as pressed KBr pellets using a Perkin-Elmer FT-IR spectrophotometer in the range of 400-4000 cm-1. The ^{1}H NMR and ^{13}C NMR were obtained using Bruker AM-500 instrument at 500 and 125 MHz respectively. UV-Vis spectra were recorded using a Perkin Elmer Lambda 35 spectrophotometer operating in the range of 200-900 nm with quartz cells and ε are given in $M^{-1}cm^{-1}$. The emission spectra were recorded on Perkin Elmer LS-45 fluorescence spectrometer. Viscosity measurements were recorded using a Brookfield Programmable LV DVII+ viscometer. The electro spray mass spectra were recorded on a Q-TOF micro mass spectrometer. Circular dichoric spectra of CT-DNA were obtained using a JASCO J-715 spectropolarimeter equipped with a Peltier temperature control device at 25 ± 0.1°C with 0.1 cm path length cuvette.

2.2 Synthesis of Schiff base ligand L

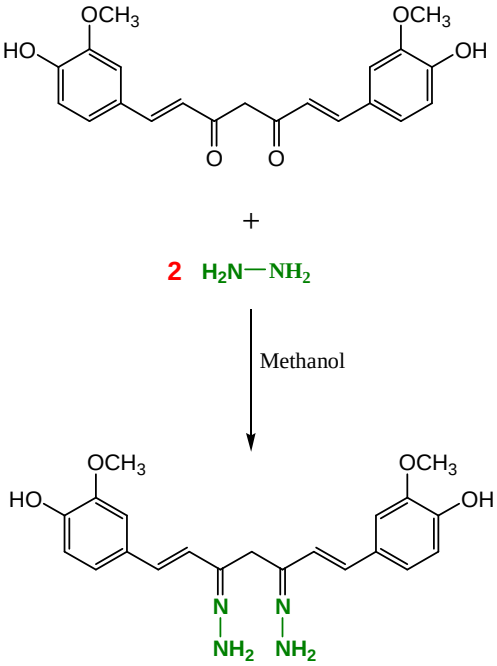

A methanolic solution (20 mL) of hydrazine hydrate (0.002 mol, 0.270 gm) was slowly added to a methanolic solution (20 mL) of curcumin (1 gm, 0.0054 mol) with constant stirring as shown in Scheme 1. This reaction

mixture was stirred for 6 h, and then refluxed for 8 h on water bath. Removal of solvent at reduced pressure gave the crude product. The product was washed twice with diethyl ether and recrystallized from chloroform.

2.3 Synthesis of Schiff base ligand L1 and its metal complexes

A methanolic solution (20 mL) of ligand L (0.0025 mol 1 gm) was slowly added to a methanolic solution (20 mL) of salicylaldehyde (0.6 gm, 0.0050 mol) with constant stirring as shown in Scheme 2. This reaction mixture was stirred for 6 h, and then refluxed for 8 h on water bath. Removal of solvent at reduced pressure gave the crude product. The product was washed twice with diethyl ether and recrystallized from chloroform.

All complexes were synthesized using the same procedure as given below:

A methanolic solution (20 mL) of ligand (L) (1.0 gm, 0.0020 mol) was added slowly to an equimolar amount of appropriate metal chloride salts in methanol (20 mL) with constant stirring. The mixture was stirred for 4 h, and the reaction was carried out for 6 h under reflux as represented in Scheme 2. After cooling the reaction mixture to room temperature, the resulting product was washed with diethyl ether and dried in vacuo.

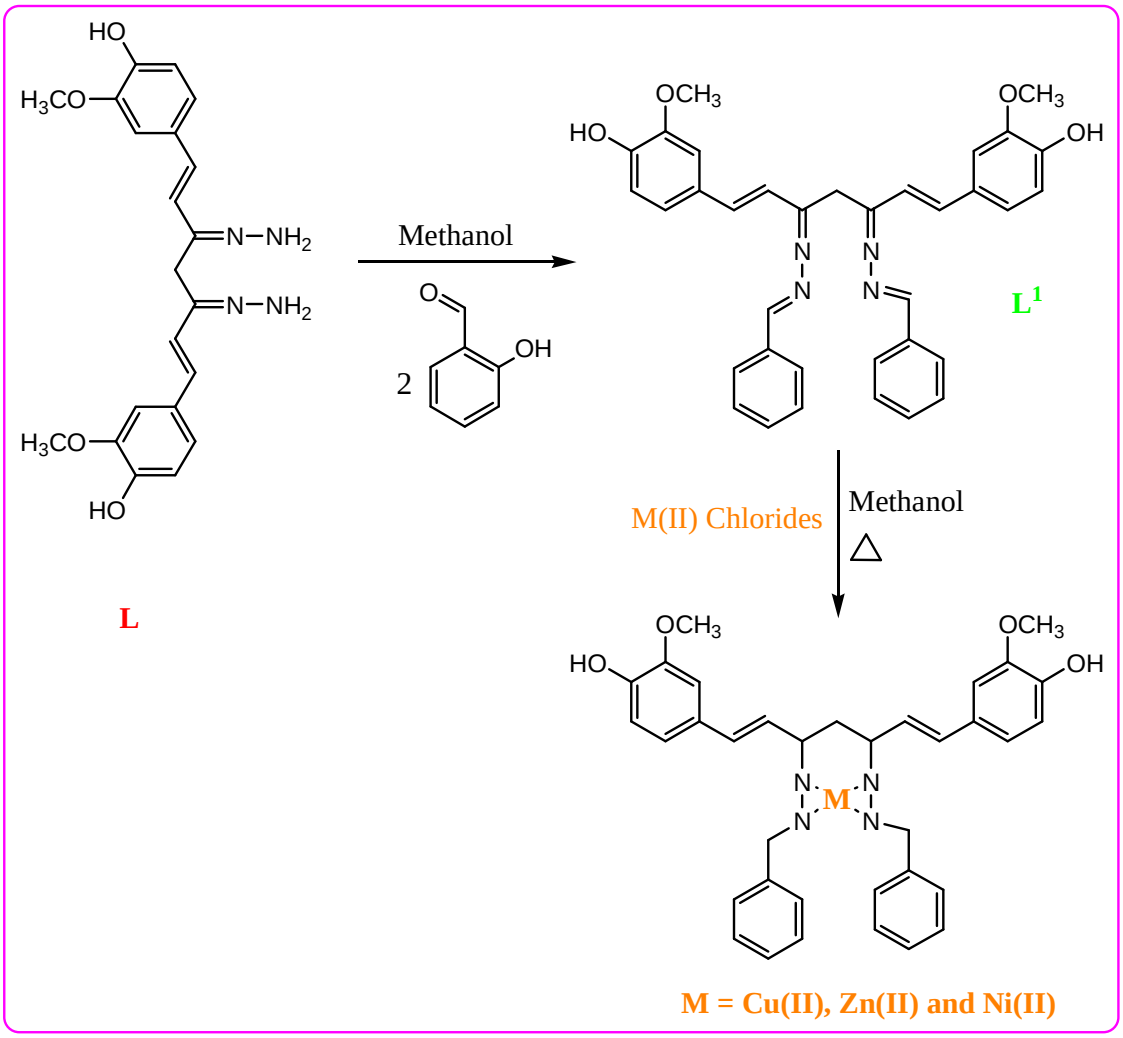

2.4 DNA binding experiments

2.4.1 Absorption spectral studies

Absorption titration experiments were performed by varying the concentration of CT-DNA (0, 40, 80, 120, 160, 200, 300 and 400 µM) while keeping the drug and its metal complexes concentration constant (40 µM). The reference solution was the corresponding buffer solution. Upon measuring the absorption spectra, an equal amount of CT-DNA solution was added to both the compound solution and the reference solution to eliminate the absorbance of DNA itself. The solutions were allowed to incubate for 10 min at room temperature before the absorption spectra were recorded. Each sample solution was scanned in the range of 200– 400 nm. The titration processes were repeated until no change in the spectra, indicating binding saturation had been achieved. The

equilibrium binding constant (Kb) values for the interaction of the complex with CT-DNA were obtained from absorption spectral titration data using the following equation (1) [13].

$$[DNA]/ (\varepsilon_a - \varepsilon_f) = [DNA]/ (\varepsilon_b - \varepsilon_f) + 1/K_b (\varepsilon_b - \varepsilon_f) \quad (1)$$

Where εa is the extinction coefficient observed for the charge transfer absorption at a given DNA concentration, εf the extinction coefficient at the complex free in solution, εb the extinction coefficient of the complex when fully bound to DNA, Kb the equilibrium binding constant, and [DNA] the concentration in nucleotides. A plot of [DNA]/ (εa - εf) versus [DNA] gives Kb as the ratio of the slope to the intercept. The non-linear least square analysis was performed using Origin lab, version 6.1.

2.4.2 Fluorescence emmission spectral studies

The emission spectrum is obtained by setting the excitation monochromator at the maximum excitation wavelength and scanning with emission monochromator. Often an excitation spectrum is first made in order to confirm the identity of the substance and to select the optimum excitation wavelength. Further experiments were carried out to gain support for the mode of binding of complexes with CT-DNA. Non-fluorescent or weakly fluorescent compounds can often be reacted with strong fluorophores enabling them to be determined quantitatively. On this basis molecular fluorophore Ethidium Bromide was used which emits fluorescence in presence of CT-DNA due to its strong intercalation. Quenching of the fluorescence of EthBr bound to DNA were measured with increasing amount of metal complexes as a second molecule and Stern–Volmer quenching constant K_{sv} was obtained from the following equation [14].

$$I_o/I=1 + K_{svr}. \quad (2)$$

Where I_0, is the ratio of fluorescence intensities of the complex alone, I is the ratio of fluorescence intensities of the complex in the presence of CT-DNA. Ksv is a linear Stern – Volmer quenching constant and r is the ratio of the total concentration of quencher to that of DNA, [M] / [DNA]. A plot of I_0 / I vs. [complex]/ [DNA], Ksv is given by the ratio of the slope to the intercept. The apparent binding constant (K_{app}) was calculated using the equation K_{EB}[EB] / K_{app}[complex], where the complex concentration was the value at a 50% reduction of the fluorescence intensity of EB and K_{EB} = 1.0 x 10^7 M^{-1} ([EB] = 3.3 μM).

2.4.3 CD spectral studies

Circular dichroic spectra of CT DNA in the presence and absence of metal complexes were obtained by using a JASCO J-715 spectropolarimeter equipped with a Peltier temperature control device at 25 ± 0.1 °C with a 0.1 cm path length cuvette. The spectra were recorded in the region of 220–320 nm for 200 μM DNA in the presence of 100 μM of the complexes.

2.4.4 Viscosity measurements

To find the binding mode of the complexes towards CT-DNA, viscosity measurements were carried out on CT-DNA (0.5 mM) by varying the concentration of the complexes (0.01 mM, 0.02 mM, 0.03 mM, 0.04 mM, 0.05 mM). Data were presented as (η/ηo) versus binding ratio of concentration of complex to that of concentration of CT-DNA , where η is the viscosity of DNA in the presence of complex and ηo is the viscosity of DNA alone.

RESULTS

3.1 Structural characterization of the Schiff base ligand

3.1.1 FT-IR spectral analysis

In order to find binding modes of Schiff base ligands and salicylaldehyde with transition metal ions, IR spectra of compounds were recorded. The IR spectra of the ligand L showed a broad band in the region 3473 cm^{-1}, assignable to intra-molecular hydrogen bonded –OH groups. The phenyl group shows C–H stretching at 3026 cm^{-1}. In the spectra of Schiff base ligand and their complexes, disappearance of carbonyl band and a new strong sharp band that appears at 1642 cm^{-1} region is attributed to the ν(C=N) band, confirming the formation of the Schiff base ligand. The spectrum of the ligand L and L1 shows–C=N bands in the region 1640 cm^{-1}, which is shifted to lower frequencies in the spectra of the complexes 1621 cm^{-1} indicating the involvement of –C=N nitrogen in coordination to the metal ion. In order to study the bonding mode of Schiff base to the metal complexes, the IR spectrum of the free ligand is compared with the spectra of the complexes. Assignment of the proposed coordination sites is further supported by the appearance of medium bands around 512 cm^{-1} which could be attributed to ν M–N. The IR spectra of metal complexes are like to each other, except for slight shifts and intensity changes of few vibration peaks caused by different metal(II) ions, which indicate that the complexes have similar structure. The representative spectra of the ligand and the metal complexes are shown in Figure 1, 2 and Figure S1.

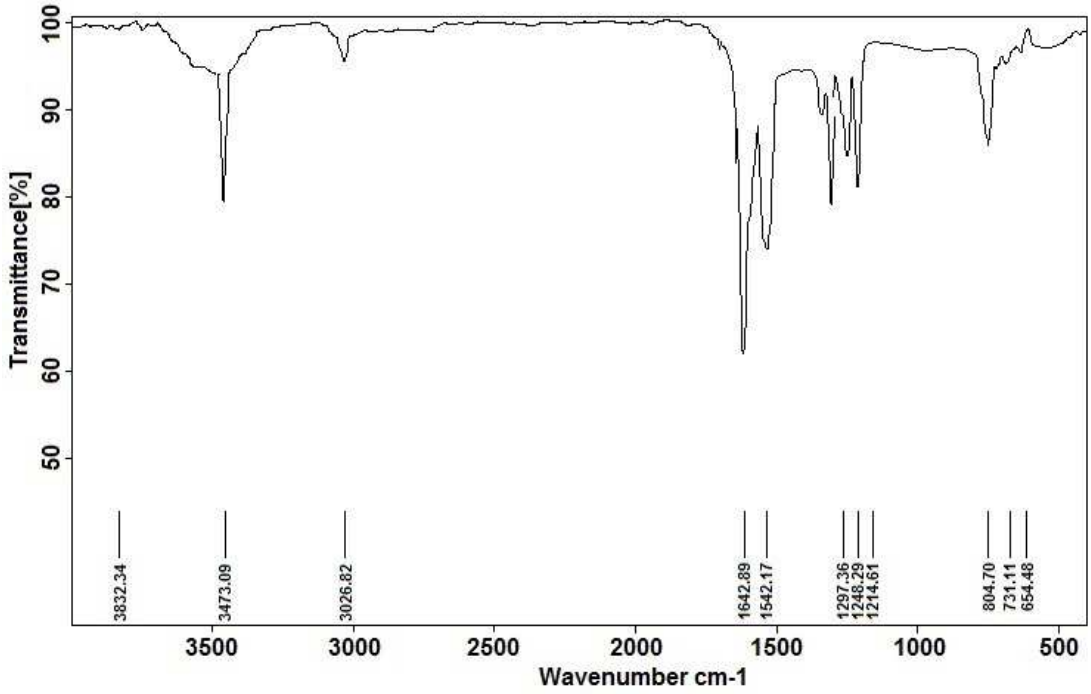

Figure 1. FT-IR spectrum of the Schiff base ligand (L)

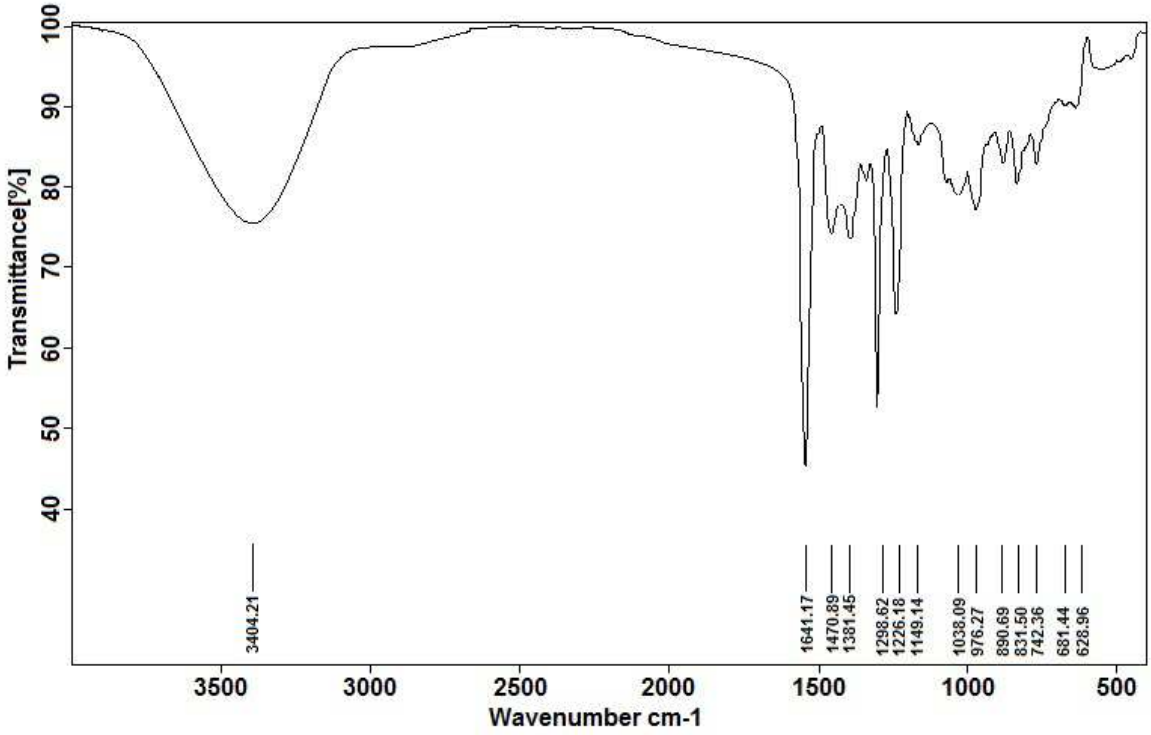

Figure 2. FT-IR spectrum of the Schiff base ligand (L1)

3.1.3 Mass spectral analysis:

The molecular ion peak [M^+] at m/z = 396 confirms the molecular weight of the Schiff base ligand L $C_{21}H_{24}N_4O_4$. The peaks at m/z = 366, 288, 232, 192, 154 and 124 corresponds to the various fragments $C_{20}H_{22}N_4O_3$, $C_{15}H_{20}N_4O_2$, $C_{12}H_{16}N_4O$, $C_{10}H_{16}N_4$, $C_7H_{14}N_4$ and $C_7H_{12}N_2$ respectively as shown in Figure 3. This confirms the molecular structure of the ligand L. The molecular ion peak [M^+] at m/z = 604 confirms the molecular weight of the Schiff base ligand L1 $C_{35}H_{32}N_4O_6$. The peaks at m/z = 512, 450, 374, 332, 216, 160 and 78 corresponds to the various fragments

$C_{33}H_{28}N_4O_6$, $C_{28}H_{26}N_4O_2$, $C_{22}H_{22}N_4O_2$, $C_{21}H_{24}N_4$, $C_{14}H_{20}N_2$ and $C_{10}H_{12}N_2$ and C_6H_6 respectively as shown in Figure S2. This confirms the molecular structure of the ligand L1.

The molecular ion peak [M^+] at m/z = 672 confirms the molecular weight of the Schiff base Cu (II) complex $C_{35}H_{36}N_4O_6Cu$. The peaks at m/z = 579, 455, 404, 376, 269 and 163 corresponds to the various fragments $C_{33}H_{32}N_4O_2Cu$, $C_{23}H_{28}N_4O_2Cu$, $C_{19}H_{24}N_4O_2Cu$, $C_{17}H_{20}N_4O_2Cu$, $C_{10}H_{14}N_4OCu$ and $C_3H_8N_4Cu$ respectively as shown in Figure 4. The molecular ion peak [M^+] at m/z = 667 and 674, confirms the molecular weight of the Schiff base Zn(II) and Ni(II) complex $C_{35}H_{36}N_4O_4M$ [M = Zn and Ni]. The type of fragmentation observed in Zn(II) and Ni(II) complex was similar with that of the Cu(II) complex. The mass spectra of the Zn(II) and Ni(II) complexes is depicted in Figure S3 and S4.

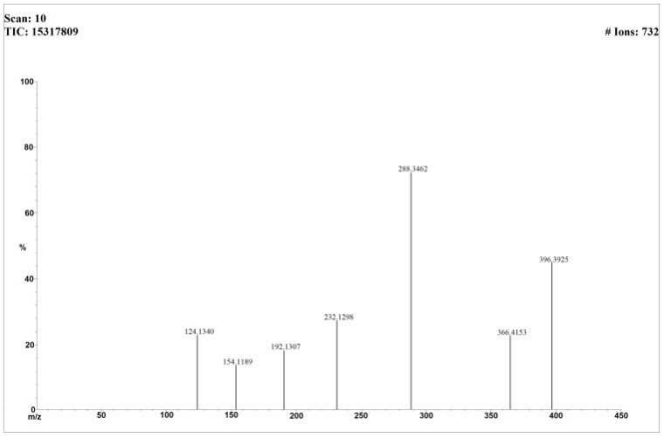

Figure 3. ESI-Mass spectrum of Schiff base ligand (L)

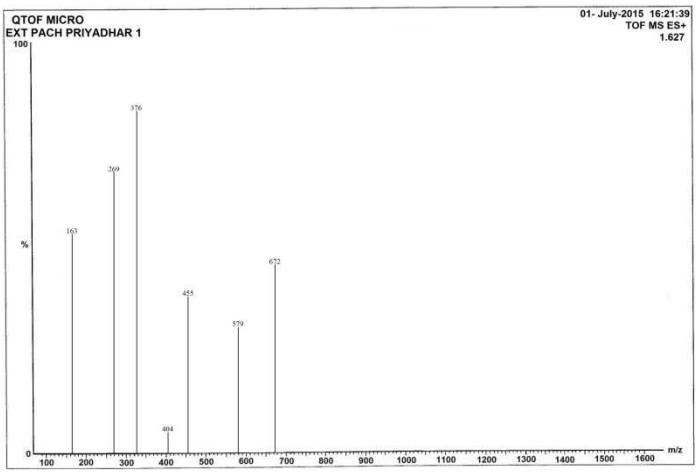

Figure 4. ESI-Mass spectrum of Cu(II) complex

3.1.2 Uv-vis spectral analysis:

The electronic spectra of the ligand and their respective complexes were recorded in DMSO at room temperature. In the spectrum of the ligand as shown in Figure 5a, the band in the 370 nm range are assigned to the n-π* transitions of the azomethine group. During the formation of the complexes, these bands are shifted to lower wavelength, suggesting that the nitrogen atom of the azomethine group is coordinated to the metal ion. The values in the 250 - 300 nm range are attributed to the π-π* transition of the aromatic ring. In the spectra of the complexes, these bands are shifted slightly to lower wave length. The electronic spectrum of the Cu(II) complex in DMSO exhibits a d–d band at 690 nm (Figure 5b), which can be assigned to the combination of $^2B_{1g}$ ^2E_g and $^2B_{1g}$ $^2B_{2g}$ transitions [15] in a distorted square planar copper(II) environment. The Ni(II) complex is diamagnetic and the band around 440 nm could be assigned to $^1A_{1g}$ $^1B_{1g}$ transition, consistent with other square-planar nickel(II) complexes [16].

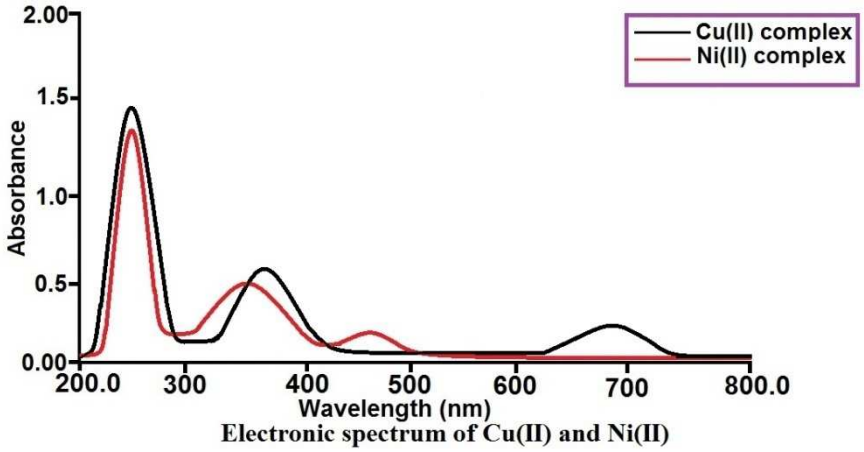

Figure 5. Electronic spectrum of the (a) ligand (L), (b) Cu(II) and Ni(II) complexes

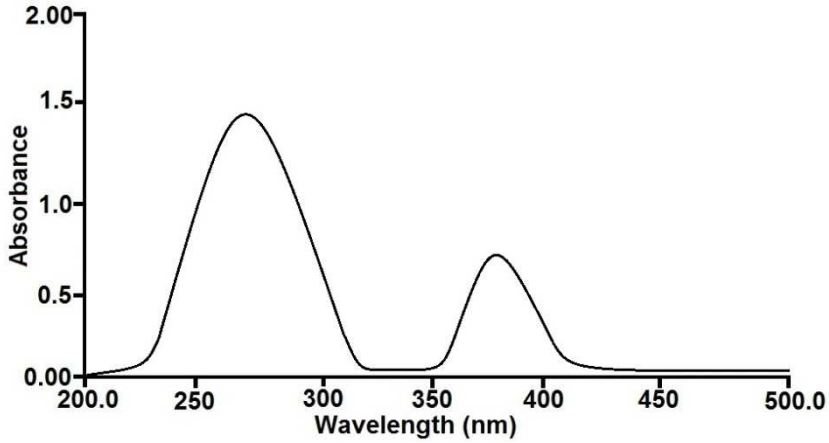

Figure 6. ^{1}H-NMR spectrum of Schiff base ligand (L)

3.1.4 NMR spectral analysis:

^{1}H NMR spectra of Schiff base ligand L showed peak at δ 1.292 ppm as singlet is due to the presence of CH_2. The six methyl protons were observed as singlet around δ 3.37 ppm. The doublets around δ 5.45 ppm are owing to the presence of ethylene protons. The NH_2 protons were observed around δ 7.43 ppm as singlet. Other peaks around δ 6.52 – 6.40 ppm as multiplet is due to the presence of protons in benzene ring. The Figure 6 shows the ^{1}H NMR spectra Schiff base ligand L. The ^{13}C NMR spectra of schiff base ligand L is depicted in Figure 7. In the spectra the peak at δ 18.7 ppm is due to the presence of CH_2 group. The peak at δ 56.2 ppm is due to the presence of methyl carbon. The peak at δ 135.9 and 139.0 ppm is due to the presence of ethylene carbon atoms. The other peaks are owing to the presence of aromatic carbons.

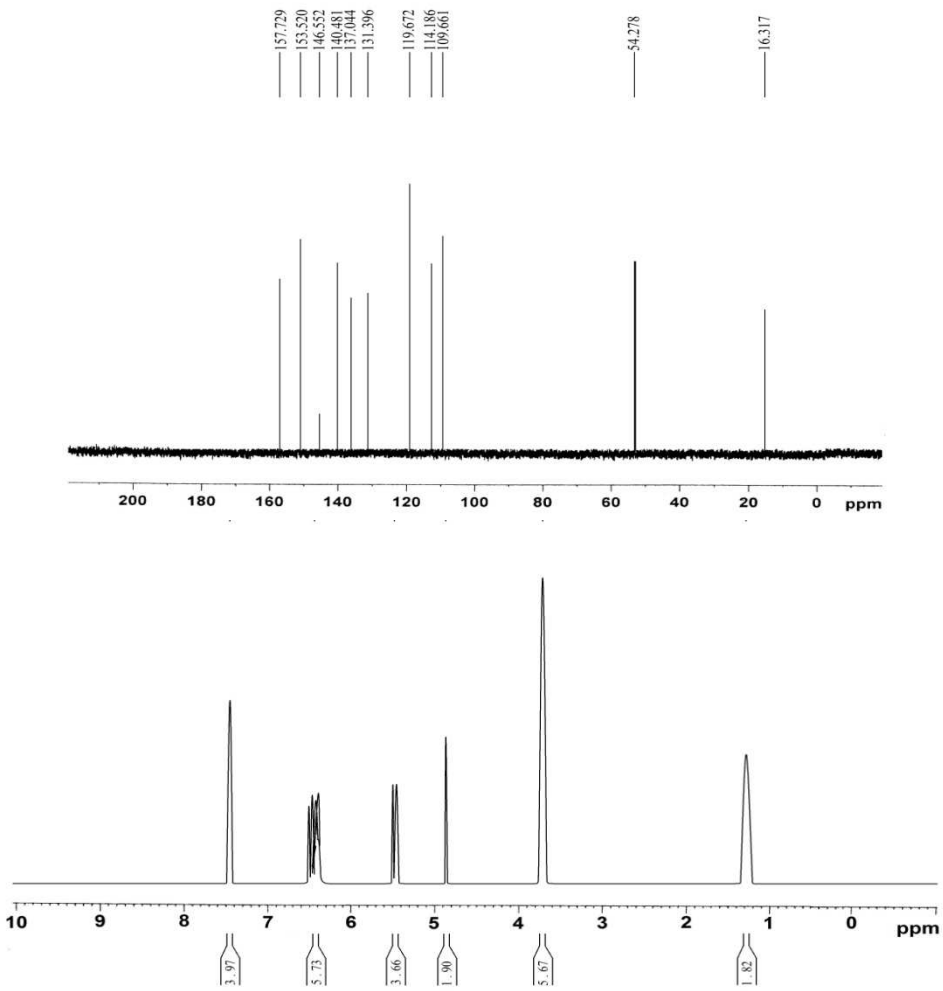

Figure 7. ^{13}C-NMR spectrum of Schiff base ligand (L).

^{1}H NMR spectra of Schiff base ligand L1 showed peak at δ 1.26 ppm as singlet is due to the presence of CH_2. The six methyl protons were observed as singlet around δ 3.46 ppm. The doublets around δ 5.56 ppm are owing to the presence of ethylene protons. Other peaks around δ 6.52 – 6.40 ppm as multiplet is due to the presence of protons in benzene ring. In the spectra the NH_2 proton was disappeared and showed a new peak at δ 8.36 ppm corresponding to imine group. The Figure S5 shows the ^{1}H NMR spectra Schiff base ligand L1. The ^{13}C NMR spectra of schiff base ligand L1 is depicted in Figure S6. In the spectra the peak at δ 18.02 ppm is due to the presence of CH_2 group. The peak at δ 54.39 ppm is due to the presence of methyl carbons. The peak at δ 129.5 and 138.2 ppm is due to the presence of ethylene carbon atoms. The other peaks are owing to the presence of aromatic carbons. Furthermore the peak at δ 168.57 is owing to the presence of imine group.

3.2 DNA binding experiments

3.2.1 Absorption spectral studies

DNA binding experiments were carried out in 0.5mL Tris–HCl/NaCl buffer [50mM Tris–HCl and 5mM NaCl (pH 7.2)] using DMF solution (15µL) of the complexes. Absorption titration measurements were done by varying the concentration of CT DNA but keeping the metal complex concentration as constant. The representative absorption spectra of Cu(II) complex in presence and absence of CT-DNA are shown in Figure 8. The absorption spectra of other complexes are given in supplementary file (Figure S7and S8). The binding mode of complexes to CT-DNA helix has been followed through absorption spectral titrations. With increasing concentration of CT-DNA the absorption bands of the complexes were affected resulting in the tendency of hypochromism and a minor red shift was observed in all the complexes. Complex binding with DNA through intercalation usually results in hypochromism and blue shift, due to the intercalative mode involving a strong stacking interaction between an aromatic chromophore and the base pairs of DNA. The extent of the hypochromism commonly parallels the

intercalative binding strength. In order to compare quantitatively the binding strength of the copper complexes, the intrinsic binding constants K_b of the complexes with DNA were obtained by monitoring the changes in absorbance with increasing concentration of DNA. Intrinsic binding constants K_b of complexes of are obtained as 5.01 x 10^4 M^{-1}, 4.61 x 10^4 M^{-1} and 4.38 x 10^4 M^{-1} respectively. The significant difference in DNA-binding affinity of the three metal(II) complexes could be understood as a result of the fact that the complex with higher numbers of metal(II) chelates showed stronger binding affinity with DNA. Our results are consistent with earlier reports on preferential binding to CT-DNA in the metal complexes [17].

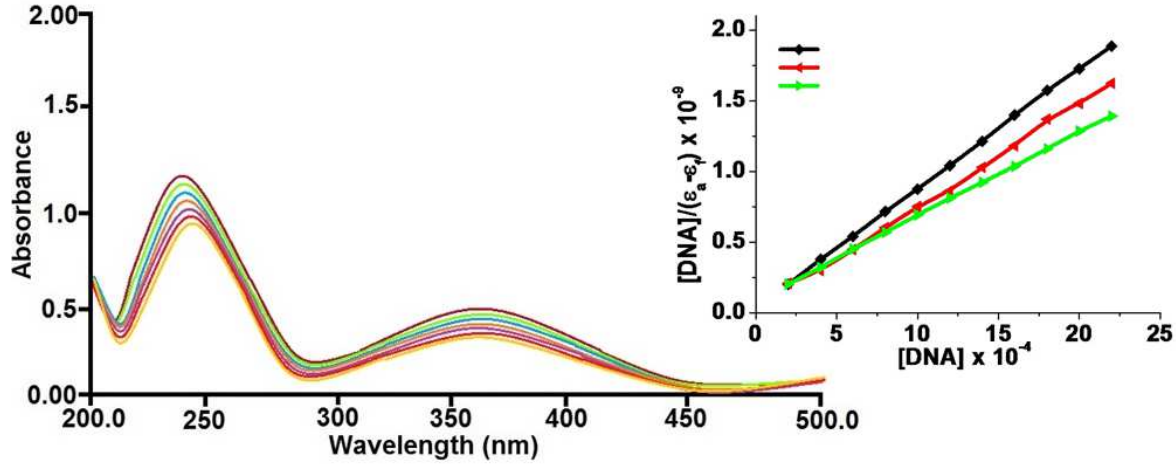

Figure 8. Absorption spectra of complex Cu(II) (1 x 10^{-5} M) in the absence and presence of increasing amounts of CT-DNA (0-2.5 x 10^{-3} M) at room temperature in 50 mM Tris-HCl / NaCl buffer (pH = 7.5). The Inset shows the plots of [DNA] / (ϵ_a-ϵ_f) versus [DNA] for the titration of DNA with Cu(II), Ni(II) and Zn(II) complexes.

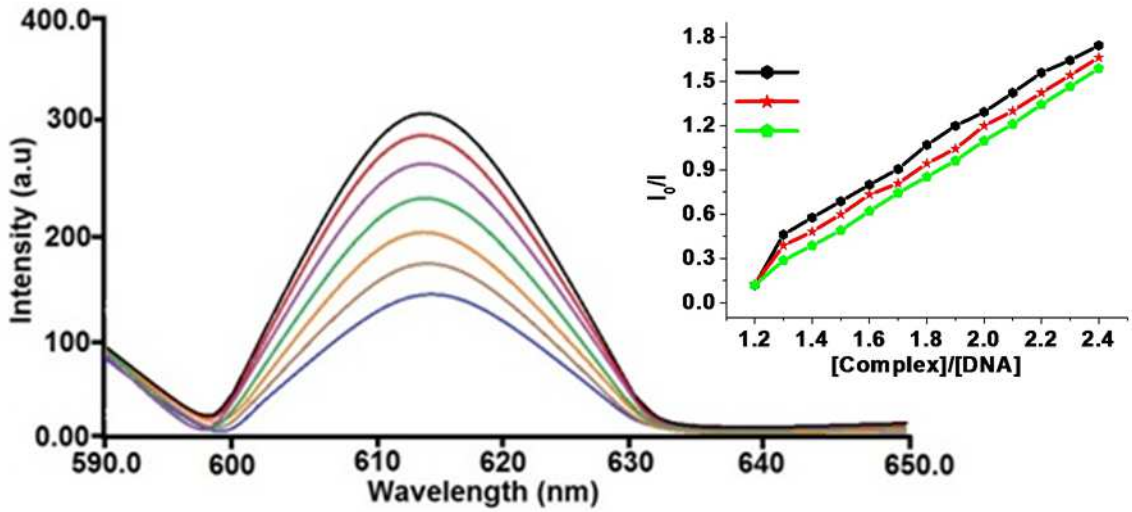

Figure 9. Emission spectrum of EB bound to DNA in the presence of Cu(II): ([EB] = 3.3 µM, [DNA] = 40 µM, [complex] = 0-25 µM, λex= 440 nm). Inset shows the plots of emission intensity I_o / I *vs* [DNA] / [complex] for the titration of DNA with Cu(II), Ni(II) and Zn(II) complexes.

3.2.2 Emission spectral studies

In order to further study the binding properties of the complexes with DNA, competitive binding experiment was carried out. Relative binding activity of the complexes towards CT-DNA was studied by the fluorescence spectral method using ethidium bromide (EB) bound CT-DNA solution in Tris–HCl/NaCl buffer (pH = 7.2). As a typical indicator of intercalation, EB is a weakly fluorescent compound. But in the presence of DNA, emission intensity of EB is greatly enhanced because of its strong intercalation between the adjacent DNA base pairs [18]. In general, measurement of the ability of a complex to affect the intensity of EB fluorescence in the EB-DNA adducts allows determination of the affinity of the complex for DNA, whatever the binding mode may be. If a complex can displace EB from DNA, the fluorescence of the solution will be reduced due to the fact that free EB molecules are readily quenched by the solvent water [19]. In the experiment, when the Zn(II)Mn(II) complex was added to the EB-DNA

system, the emission intensity was reduced. The emission spectra of EB bound to DNA in the absence and presence of the complexes are given in Figure 9, Figure S9 and S10. It can be noted that the fluorescence intensity of the EB-DNA solutions decreases with the addition of the complex obviously. The results suggest that the complex can replace the EB and bind to the DNA molecule. The quenching plots (insets in Figure 9) illustrate that the fluorescence quenching of EB bound to DNA by Cu(II), Ni(II) and Zn(II) complexes in linear agreement with the Stern–Volmer equation, which confirms that the complexes bound to DNA. The K_{app} values for Cu(II), Ni(II) and Zn(II) complexes are found to be 6.04 x 10^5 M^{-1}, 5.72 x 10^5 M^{-1} and 5.46 x 10^5 M^{-1}.–respectively. The attained results are in consistent with that of absorption spectroscopic studies. Anyway, it may be concluded that the entire complexes bound to DNA via the similar mode and the quenching constants of the synthesized complexes reveals that the interaction of the compound with DNA should be intercalation [20].

3.2.3 Viscosity studies

Viscosity, sensitive to volume increases, is regarded as the one of the least ambiguous and the most critical tests of binding interactions with DNA in solution in the absence of crystallographic structural data.In order to confirm the binding mode of the present complexes, the viscosity measurements were carried out on CT-DNA by varying the concentration of added complex. The effect of Ni(II), Co(II) and Cu(II) complexes on the viscosity of DNA is depicted in As shown in Figure 10, the specific viscosity of the DNA increases obviously with increased concentration of the complex. This again suggests that the binding mode between the complex and DNA should be a classical intercalation mode [21, 22].

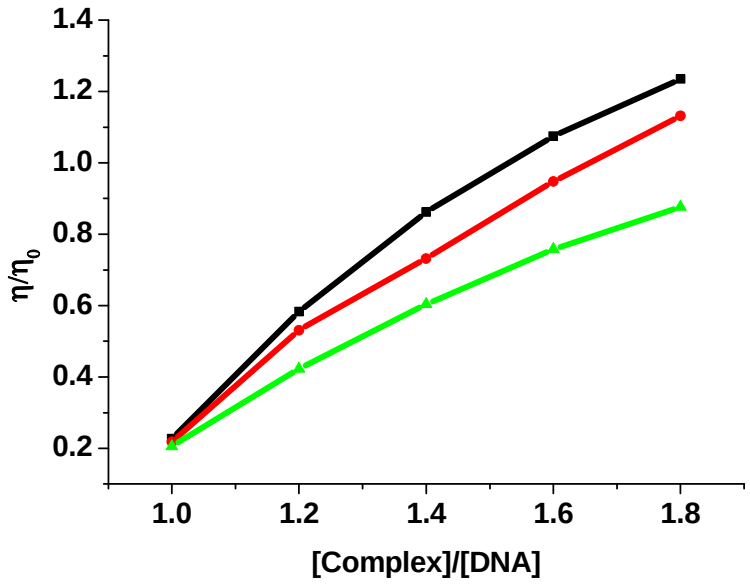

Figure 10. Viscosity measurements of the Cu(II), Ni(II) and Zn(II) complexes.

3.2.4 Circular dichoric spectral studies

The conformational changes of CT-DNA induced by the synthesized complexes were monitored by CD spectroscopy in buffer at room temperature (Figure 11). The positive band at 275 nm and the negative one at 245 nm in the CD spectrum are due to the base stacking and the right-handed helicity of B-DNA, respectively [23]. On addition of complexes to DNA solutions, perturbations in ellipticity of the two bands on the CD spectra of DNA are observed as represented in Figure 10, which reveal the effect of the complexes on base stacking and right-handedness of CT DNA as well. Without significant red shift or blue shift, there was a decrease in the negative band and increase in the positive bands their intensities. The increased intensity in the positive band may be due to the intercalation of the complexes has effect on the π-π stacking of DNA base pairs. The decreased intensity in the negative band suggests that the complexes can unwind the DNA helix and lead to some loss of helicity, which induces a more A-like conformation in DNA [24-26]. More significant changes for the negative band indicate that the complexes may have a more evident effect on the helicity of B-DNA than on the base stacking. These changes suggest that the stacking mode and the orientation of base pairs in DNA were disturbed with the binding of the complexes, and certain conformational changes, such as the conversion from a more B-like to a more A-like structure within the DNA molecules happened. These observations clearly indicate that the binding mode of the complexes should be intercalative, the stacking of the complex molecules between the DNA base pairs leads to an enhancement in the positive band and the partial unwinding of the helix decreases intensity of the negative band. So, the main interactions of the complexes with DNA can be ascribed to the intercalative mode.

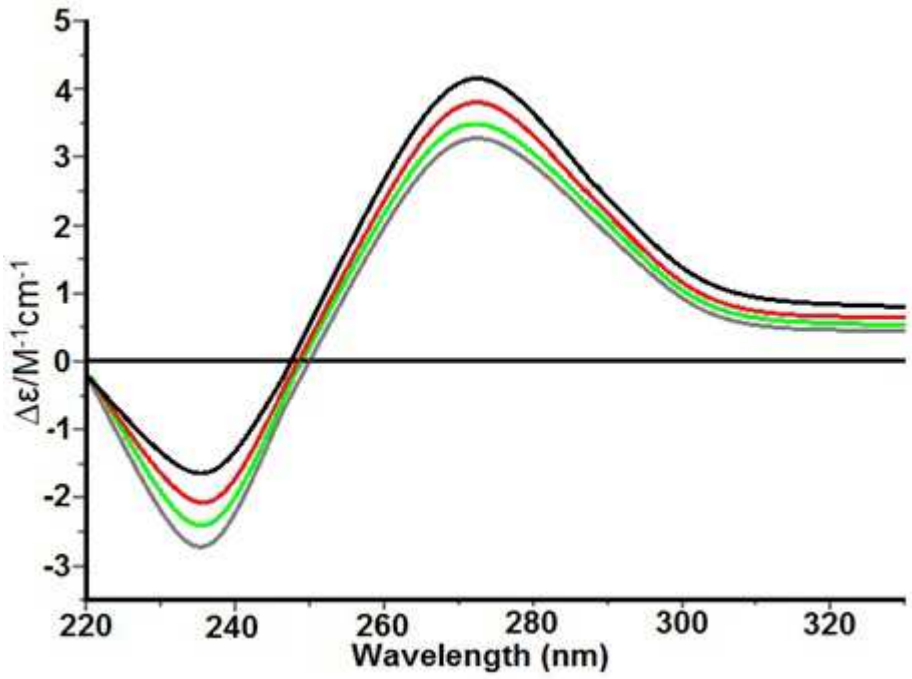

Figure 11. CD spectra recorded over the wavelength range 220-320 nm for solutions containing 2:1 ratio of CT-DNA (200 µM) and Cu(II), Ni(II) and Zn(II) complexes (100 µM).

CONCLUSION

In conclusion, we have successfully synthesized three new transition metal hydrazone complexes and characterised using various spectroscopic methods like FT-IR, NMR, UV-vis and Mass spectra. The DNA binding of metal complexes examined by absorption and fluorescence spectral techniques revealed an intercalative interaction between them and CT-DNA with binding constants ranging from 10^3-10^5 M^{-1}. Among the investigated complexes, the one containing copper as the central metal ion showed better binding affinity than the other two complexes containing Zinc and nickel ions as metal counterparts respectively.

REFERENCES

[1] C.S. Dilip, V.S. Kumar, S.J. Venison, I.V. Potheher, D.R. Subahashini, *J. Mol. Struct*. 1040 (**2013**) 192.
[2] N, Raman, R. Mahalakshmi, L. Mitu, *Spectrochim Acta A Mol Biomol Spectrosc* 131 (**2014**) 355.
[3] K. Abdi, H. Hadadzadeh, M. Weil, M. Salimi, *Polyhedron* 31 (**2012**) 638.
[4] J. G. Liu, B. H. Ye, H. Li, Q. X. Zhen, L.N. Ji, Y. H. Fu, *J. Inorg. Biochem*. 76 (**1999**) 265.
[5] L. M. Chen, J. Liu, J. C. Chen, S. Shi, *J, Mol. Struct*. 881 (**2008**) 156.
[6] D. Pucci, T. Bellini, A. Crispini, I. D'Agnano, P. F. Liguori, P. Garcia-Orduna, S. Pirillo, A. Valentinid, G. Zanchetta, *Med. Chem. Commun*. 3 (**2012**) 462.
[7] B. M. Z eglis, V. C. Pierre, J. K. Barton, *Chem. Comm*. (**2007**) 4565.
[8] A. Mukherjee, R. Lavery, B. Bagchi, J. T. Hynes, *J. Am. Chem. Soc*. 130 (**2008**) 9747.
[9] M. A. Ali, R. N. Bose, *Polyhedron* 3 (**1984**) 517.
[10] C. Richardson, P. J. Steel, *Inorg. Chem. Comm*. 10 (**2007**) 884.
[11] H. Hatcher, R. Planalp, J. Cho, F.M. Torti, S.V. Torti, *Cell. Mol. Life Sci*. 65 (**2008**) 1631.
[12] J. Kim, H. J. Lee, K.W. Lee, *J. Neurochem*. 112 (**2010**) 1415.
[13] A. Wolfe, G. H. Shimer, T. Mechan, *Biochem*. 26 (**1987**) 6392.
[14] J.R. Lakowiez, G. Webber, *Biochem*. 12 (**1973**) 4161.
[15] S. Tabassum, A. Bashar, F. Arjmand, K. S. Siddiqu, *Synth. React. Inorg. Met.-Org. Chem*. 27 (**1997**) 487.
[16] C. Natarajan, P. Tharmaraj, R. Murugesan, *J. Coord. Chem*. 26 (**1992**) 205.
[17] D. D. Li, J. L. Tian, W. Gu, X. Liu, S. P. Yan, *J. Inorg. Biochem*. 104 (**2010**) 171.
[18] B. C. Baguley, M. L. Bret, *Biochem* 23 (**1984**) 937.
[19] J. B. LePecq, C. Paoletti, *J. Mol. Biol*. 27 (**1967**) 87.
[20] D. S. Raja, N. S. P. Bhuvanesh, K. Natarajan, *Inorg. Chim. Acta* 385 (**2012**) 81.
[21] J. Sun, W. Shuo, Y. An, J. Liu, F. Gao, L. N. Ji, Z. W. Mao *Polyhedron* 27 (**2008**) 2845.
[22] J. G. Liu, B. H. Ye, H. Li, Q. X. Zhen, L. N. Ji, Y. H. Fu, *J Inorg Biochem* 76 (**1999**) 265.

[23] W.C. Johnson, in: K. Nakanishi, N. Berova, R.W. Woody (Eds.), Circular Dichroism: Principles and Applications, VCH, New York, **1994**, pp. 523–540.
[24] P. U. Maheswari, M. Palaniandavar, *J.Inorg. Biochem*. 98 (**2004**) 219.
[25] H. Zou, B. H. Ye, H. Li, Q. L. Zhang, H. Chao, J. G. Liu, L. N. Ji, X. Y. Li, *J. Biol. Inorg. Chem*. 6 (**2001**) 143.
[26] Q. Cheng, Z. Pan, H. Zhou, J. Chen, *Inorg. Chem. Commun*. 14 (**2011**) 929.

Supplementary Figures:
Figure S1:

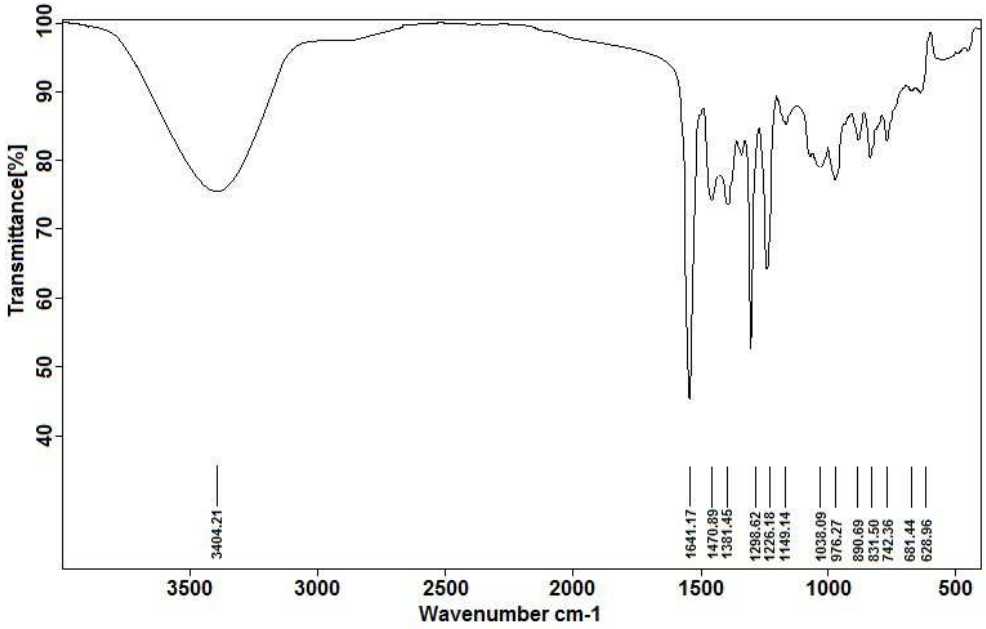

Figure S1. FT-IR spectrum of the Schiff base ligand (L1).

Figure S2:

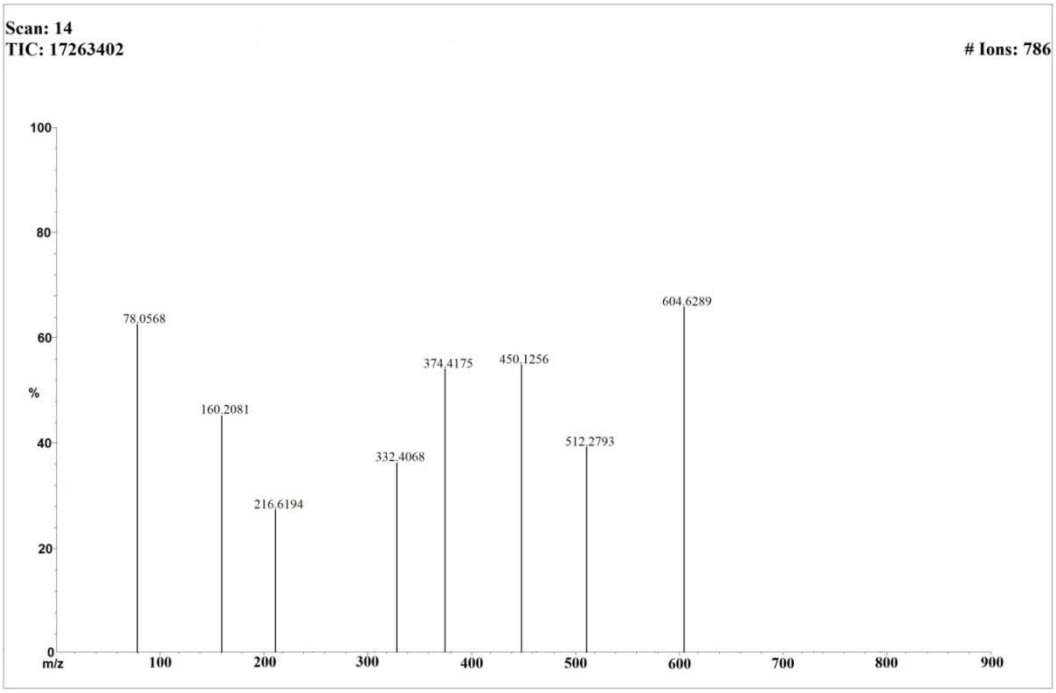

Figure S2. Mass spectrum of Schiff base ligand (L1).

Figure S3:

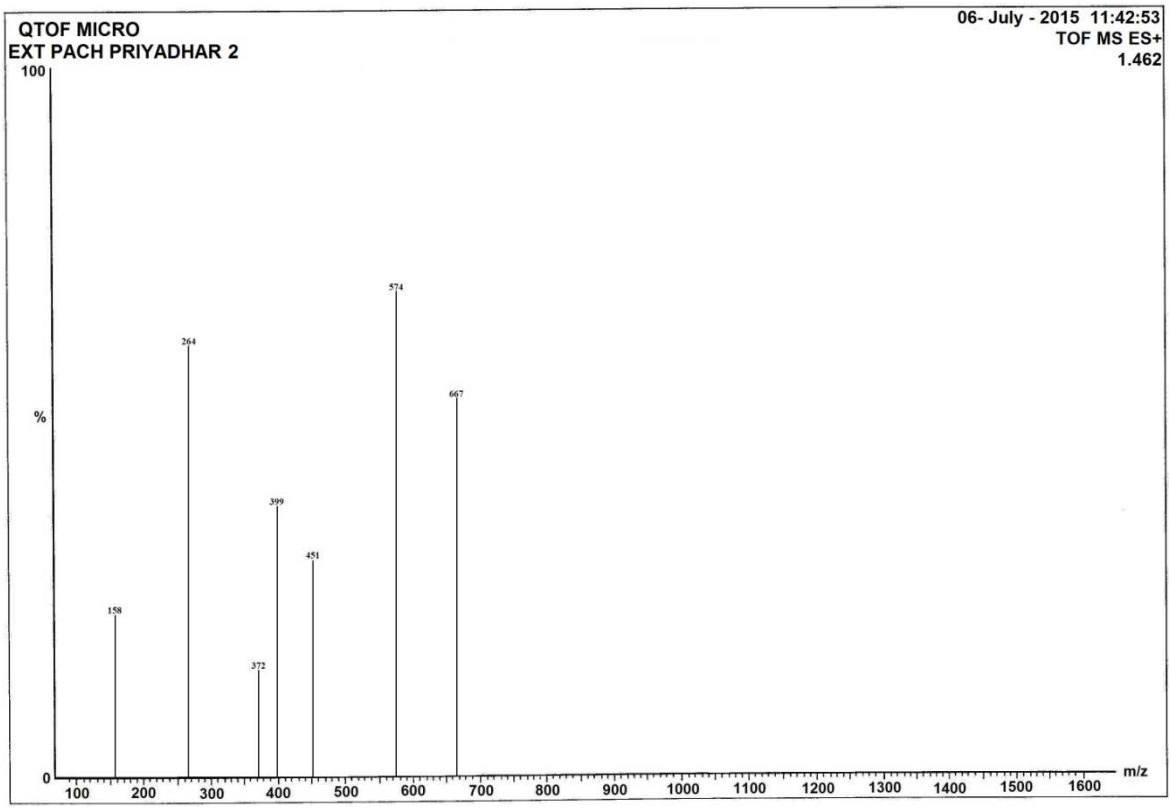

Figure S3. Mass spectrum of Ni(II) complex.

Figure S4:

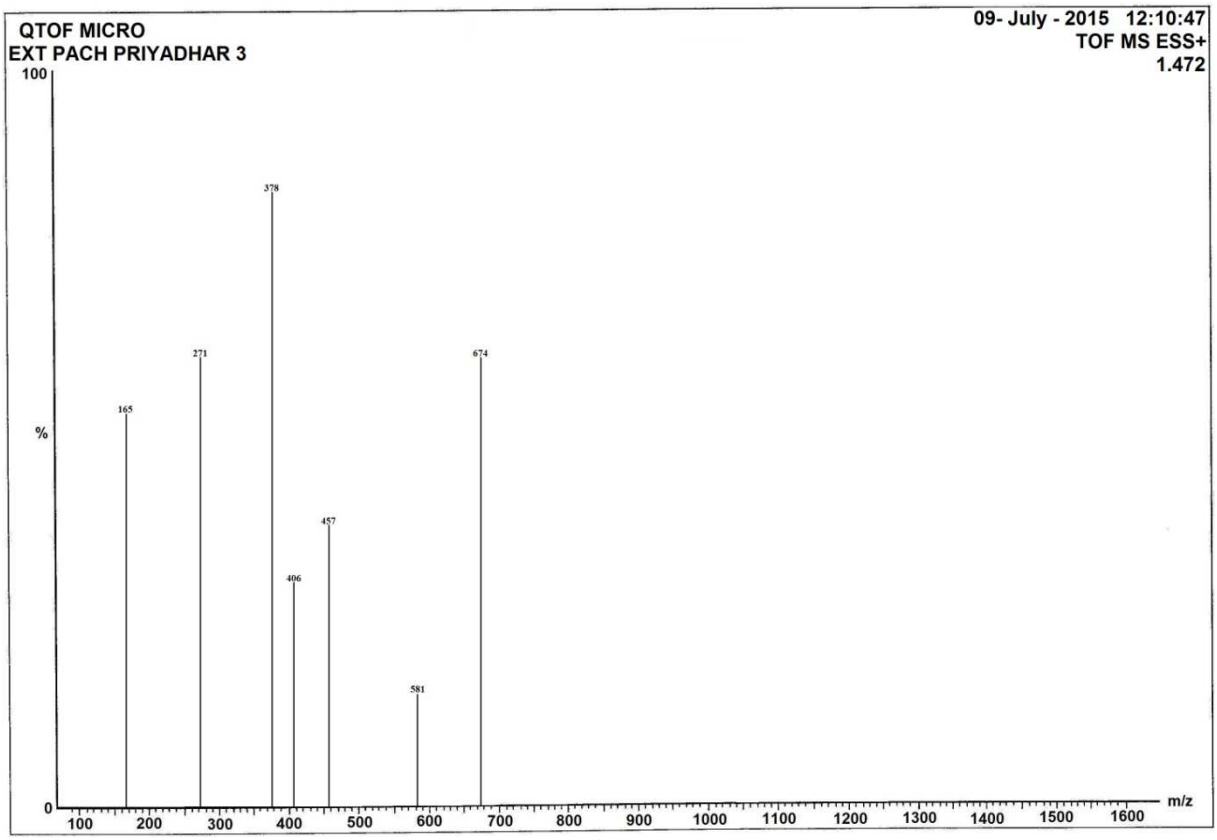

Figure S4. ESI-Mass spectrum of Zn(II) complex

Figure S5:

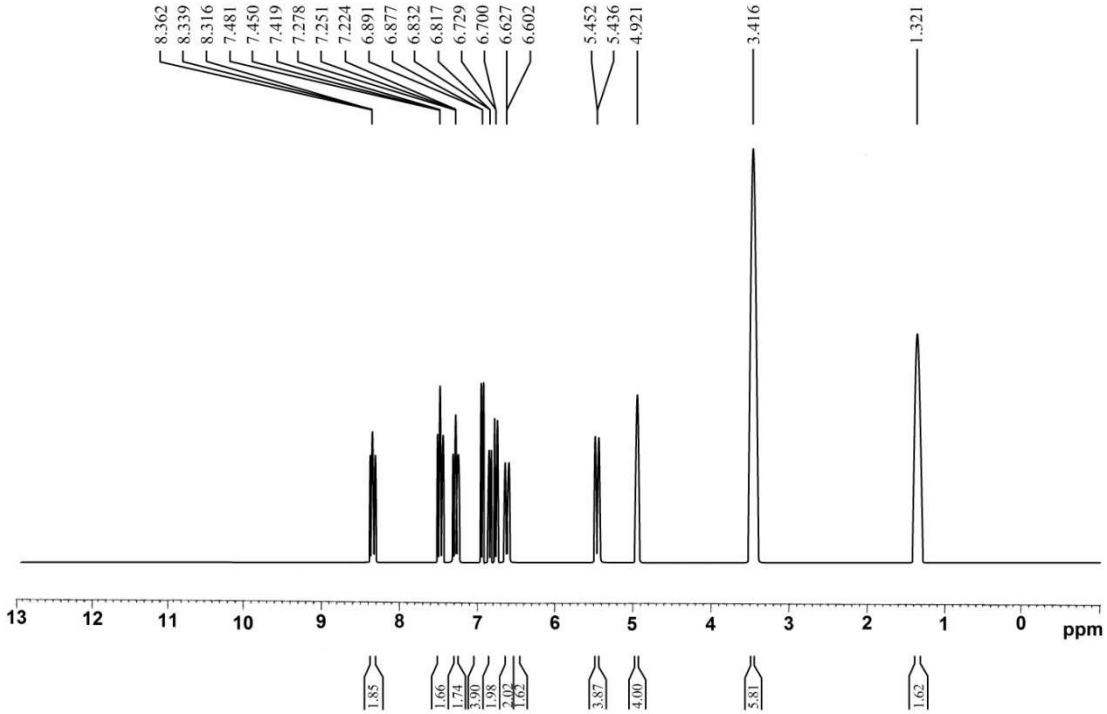

Figure S5. [1]H-NMR spectrum of Schiff base ligand (L1).

Figure S6.

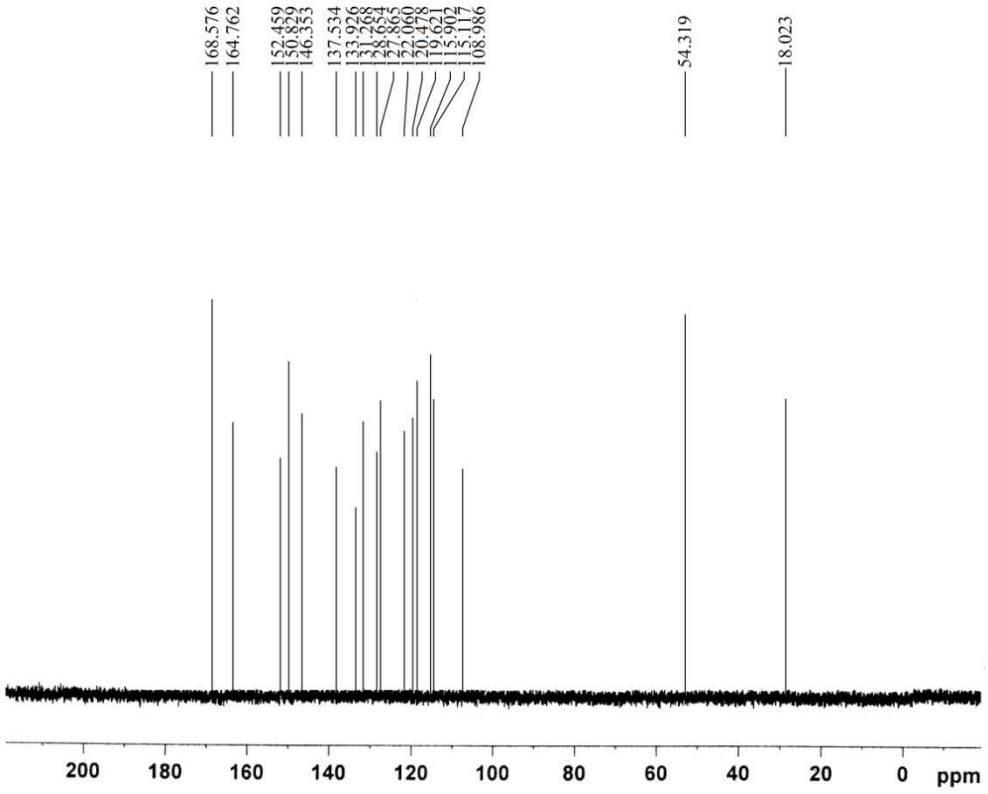

Figure S6. [13]C-NMR spectrum of Schiff base ligand (L1).

Figure S7.

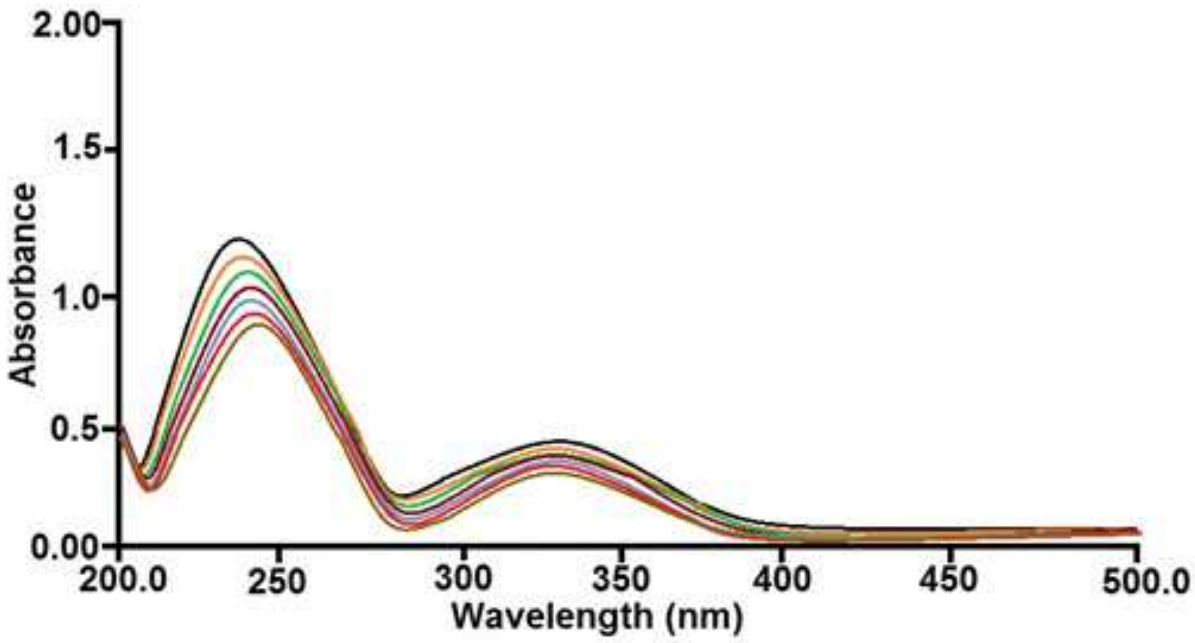

Figure S7. Absorption spectra of complexes Ni(II), (1 x 10^{-5} M) in the absence and presence of increasing amounts of CT-DNA (0-2.5 x 10^{-3} M) at room temperature in 50 mM Tris-HCl / NaCl buffer (pH = 7.5).

Figure S8.

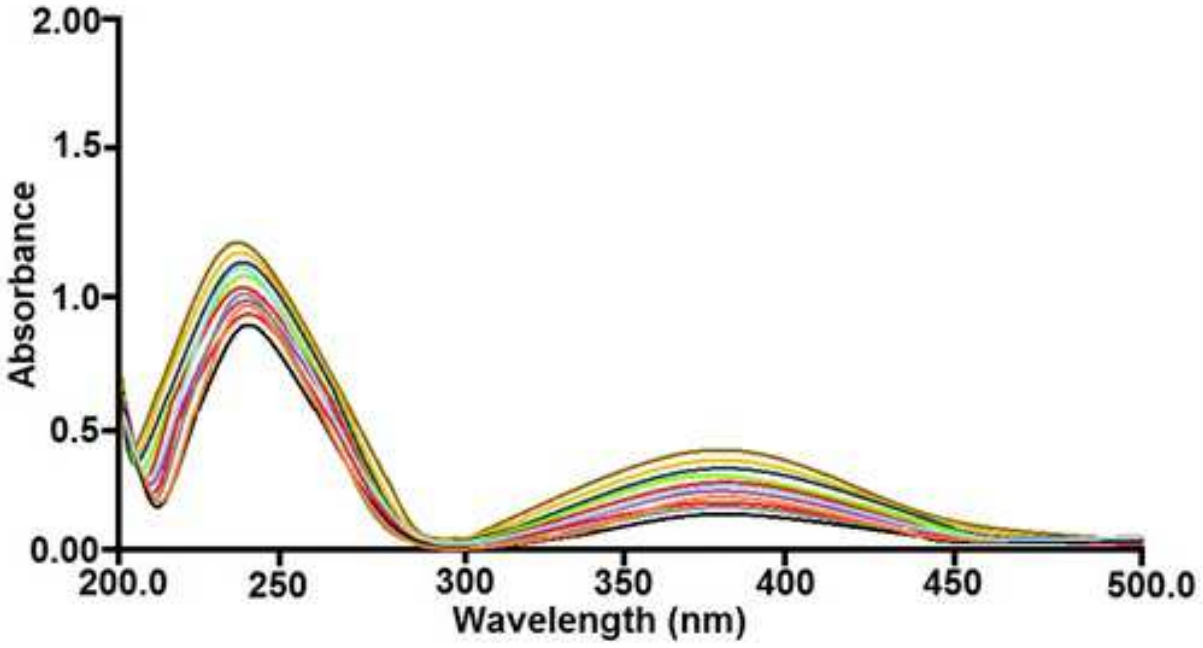

Figure S8. Absorption spectra of complexes Zn(II), (1 x 10^{-5} M) in the absence and presence of increasing amounts of CT-DNA (0-2.5 x 10^{-3} M) at room temperature in 50 mM Tris-HCl / NaCl buffer (pH = 7.5).

Figure S9.

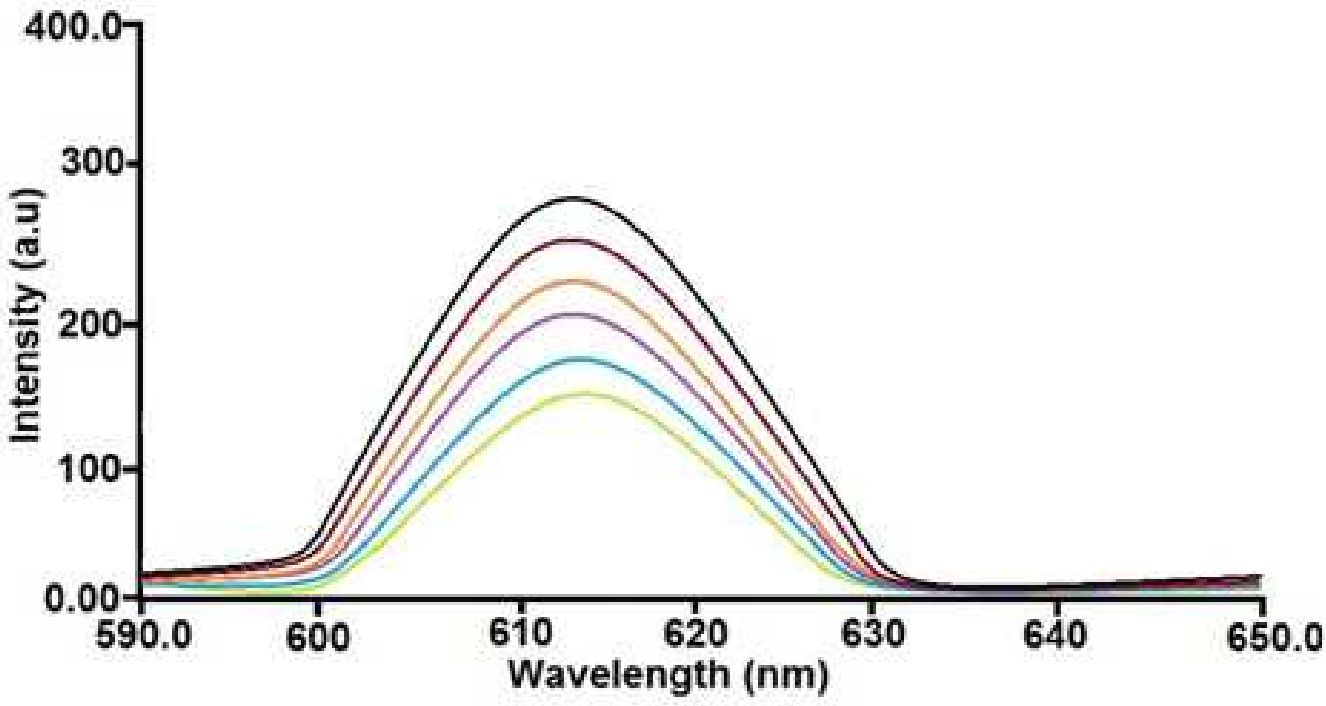

Figure S9. Emission spectrum of EB bound to DNA in the presence of Ni(II); ([EB] = 3.3 µM, [DNA] = 40 µM, [complex] = 0-25 µM, λex= 440 nm).

Figure S10.

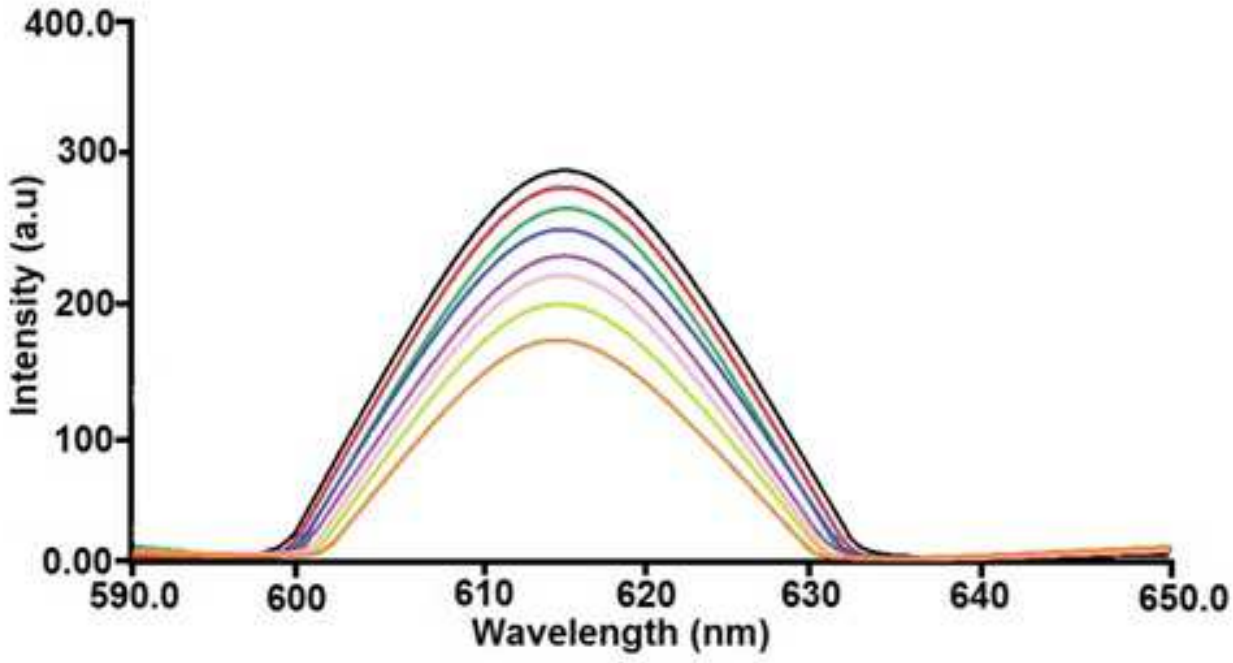

Figure S10. Emission spectrum of EB bound to DNA in the presence of Zn(II); ([EB] = 3.3 µM, [DNA] = 40 µM, [complex] = 0-25 µM, λex= 440 nm).